Non-targeted metabolomics reveals diagnostic biomarker in the plasma of patients with lung cancer

YAN LIU[1*], YANGMIN LI[2,3*], HAIJUN HOU[1], YANYAN DONG[1], HAITONG TIAN[4], YANAN ZHAO[5], KE LI[6], JIAYUAN ZHOU[5], FUJIE SONG[4] and YAN LI[2]

[1]Department of Respiratory Medicine, Tongzhou Branch of Dongzhimen Hospital, Beijing University of Chinese Medicine, Beijing 101121, P.R. China; [2]Emergency Department, Dongzhimen Hospital, Beijing University of Chinese Medicine, Beijing 100007, P.R. China; [3]Graduate School, Beijing University of Chinese Medicine, Beijing 100029, P.R. China; [4]Department of Thoracic Surgery, Tongzhou Branch of Dongzhimen Hospital, Beijing University of Chinese Medicine, Beijing 101121, P.R. China; [5]Out-Patient Department, Tongzhou Branch of Dongzhimen Hospital, Beijing University of Chinese Medicine, Beijing 101121, P.R. China; [6]Department of Radiology, Tongzhou Branch of Dongzhimen Hospital, Beijing University of Chinese Medicine, Beijing 101121, P.R. China

Received May 30, 2025; Accepted October 13, 2025

DOI: 10.3892/ol.2025.15369

Abstract. Lung cancers are malignant tumors with high incidence and mortality rates and a 5-year survival rate that depends on the stage at the time of diagnosis. Screening methods for lung cancer are becoming increasingly diverse, but existing approaches lack sensitivity or specificity for early lesions, posing notable challenges for the early diagnosis of lung cancer. Therefore, it is essential to explore potential biomarkers with high sensitivity and specificity to achieve early diagnosis. The present study employed liquid chromatography-mass spectrometry to analyze plasma metabolic changes in patients with lung cancer or pulmonary nodules and in healthy individuals. By combining quantitative and qualitative methods, differential metabolites were identified and the performance of these metabolites was evaluated using receiver operating characteristic curve analyses to screen for potential biomarkers. A total of 50 differential metabolites, six of which had an area under the curve of >0.9, were identified among the three groups and regarded as potential biomarkers for distinguishing between lung cancer, pulmonary nodules and healthy individuals, as well as between lung cancer and pulmonary nodules. In addition, metabolic pathways were screened using the Kyoto Encyclopedia of Genes and Genomes databases. The results demonstrated that significant changes were observed in the metabolism of substances including linoleic acid, α-linolenic acid, arginine and proline, suggesting that the development of lung cancer may be associated with alterations in amino acid and lipid metabolism. In conclusion, the present findings provided potential biomarkers to differentiate between lung cancer, pulmonary nodules and healthy individuals, offering insights into the pathological mechanisms of lung cancer.

Correspondence to: Professor Yan Li, Emergency Department, Dongzhimen Hospital, Beijing University of Chinese Medicine, 5 Hu Tong, Haiyun Cang, Dongcheng, Beijing 100007, P.R. China
E-mail: 13011097949@126.com

Professor Fujie Song, Department of Thoracic Surgery, Tongzhou Branch of Dongzhimen Hospital, Beijing University of Chinese Medicine, 116 Cuiping West Road, Tongzhou, Beijing 101121, P.R. China
E-mail: songfj68@126.com

*Contributed equally

Key words: metabolomics, lung cancer, liquid chromatography-mass spectrometry, plasma metabolic biomarker, diagnostic biomarker

Introduction

Lung cancer is the most common malignant tumor and the leading cause of cancer-related mortality worldwide (1). It is estimated that there are 2.2 million novel diagnoses of lung cancer each year, as well as 1.79 million mortalities (2). Lung cancer poses a severe threat to human health, and its diagnosis and treatment have become a key focus in oncological research. However, due to the insidious early symptoms of lung cancer, ~75% patient are diagnosed at advanced stages of the disease, missing the optimal treatment window, which results in a continuous increase in the mortality rates associated with lung cancer (3,4). Therefore, early diagnosis of lung cancer is key to ensuring timely treatment and improving survival rates.

Early lung cancer often presents as pulmonary nodules on imaging (5). Therefore, recognizing malignant pulmonary nodules is key to the early diagnosis and treatment of lung cancer, as well as to reduce lung cancer-related mortality. Low-dose CT is an effective method for the detection of malignant pulmonary nodules (6), but it suffers from a high false-positive rate (7). Positron emission tomography has a certain accuracy in differentiating between benign and malignant lung nodules, but it carries a high risk of false-negatives

or false-positives (8,9). Lung tissue biopsy is the standard for lung cancer diagnosis; however, it is an invasive procedure that can lead to complications and has high costs (10). Non-invasive testing methods, such as circulating tumor cells and DNA, have demonstrated certain potential in identifying malignant pulmonary nodules, but they suffer from low capture rates and sensitivity (4,11). Tumor markers such as neuron-specific enolase, squamous cell carcinoma antigen and carcinoembryonic antigen can provide real-time assessments of tumor status and serve as an adjunct in the diagnosis of lung cancer, but they lack sensitivity and specificity (3,12). Therefore, there is an urgent need to identify a simple, non-invasive or minimally invasive, reproducible and highly sensitive method to identify diagnostic biomarkers with high sensitivity and specificity, thereby enabling the early identification of malignant pulmonary nodules.

Metabolomics is an emerging high-throughput technology used to detect, identify and quantify metabolites in biological samples. It can directly exhibit changes within seconds or minutes from an event, demonstrating high sensitivity and proving its unique value in disease diagnosis and disease mechanisms (13-15). Non-targeted metabolomics is one of the techniques in metabolomics that focuses on the comprehensive analysis of all low molecular weight metabolites. It reveals metabolic changes associated with diseases and reflects their metabolic characteristics, thus being utilized to identify potential biomarkers that provide effective assistance for disease screening and early diagnosis (15,16). Furthermore, the biological samples required for metabolomics often originate from the bodily fluids of the patients, such as blood, plasma, serum and urine (17), making sample collection convenient and repeatable, which is beneficial for routine monitoring.

Metabolic dysregulation is a hallmark of cancer occurrence and progression (18). Utilizing non-targeted metabolomics to analyze the metabolic changes from precancer to cancer helps identify potential diagnostic biomarkers. For instance, a non-targeted metabolomics study on hepatocellular carcinoma reported that PG(i-12:0/a-17:0) and phytosphingosine are potential biomarkers for early hepatocellular carcinoma diagnosis in patients with liver cirrhosis. Furthermore, norvaline, L-histidinol, N-docosahexaenoyl γ-aminobutyric acid, inosine and 3-hydroxyoctanoly carnitine revealed a high potential to distinguish patients with hepatocellular carcinoma and liver cirrhosis from normal controls (14). Currently, the main techniques in metabolomics are nuclear magnetic resonance (NMR), gas chromatography-mass spectrometry (GC-MS) and liquid chromatography-mass spectrometry (LC-MS) (19). NMR is a rapid, non-destructive and reproducible technique, but has relatively low sensitivity (19,20). GC-MS is suitable for the analysis of samples that are stable and easy to gasify but needs derivatization and a longer sample preparation time (19,20). By contrast, LC-MS has a higher sensitivity and wider testing scope, while avoiding the complex sample pretreatment in GC-MS, which makes it an increasingly predominant platform in metabolomics (19-21).

Based on the aforementioned points, in the present study, plasma samples were collected from three different stages: Patients with lung cancer, those with pulmonary nodules and healthy individuals. By analyzing the metabolic changes using LC-MS, the present study aimed to identify differential metabolites, identify potential diagnostic biomarkers for lung cancer and reveal abnormal metabolic pathways, with the intention of providing novel insights and approaches for the early diagnosis of lung cancer, as well as its pathological mechanisms in the future.

Patients and methods

Study participants. A total of 68 participants from Dongzhimen Hospital of Beijing University of Chinese Medicine (Beijing, China) were enrolled between April 2023 and May 2024, including 20 patients with lung cancer (lung cancer group), 28 patients with pulmonary nodules (pulmonary nodule group) and 20 healthy individuals (healthy group). Patients with lung cancer and pulmonary nodules were recruited using a simple random sampling method based on disease type, while healthy individuals were recruited using a matching method based on age and sex. The present study was reviewed and approved by the Ethics Committee of Dongzhimen Hospital of Beijing University of Chinese Medicine (approval no. 2022DZMEC-312-02). All methods were conducted in accordance with relevant guidelines and regulations. All participants signed informed consent forms. The inclusion criteria for lung cancer were as follows: i) The patients were confirmed to have lung adenocarcinoma through histopathological examination; ii) there were no restrictions on the sex of the patients and the age range was 18-90 years; iii) the patients had not received any treatments such as surgery, chemotherapy or radiotherapy prior to enrollment in the present study. The inclusion criteria for pulmonary nodules were as follows: i) The patient had imaging findings of round or irregularly shaped pulmonary nodules with a maximum diameter of ≤30 mm, which was either solid or subsolid in nature and exhibited increased radiological density; ii) either a) pathology results were negative or b) imaging features were benign, Lung Imaging Reporting and Data System category 2 (22) and they were classified as low-risk by the chest CT image-assisted system at Dongzhimen Hospital of Beijing University of Chinese Medicine; iii) there were no restrictions on the sex of the patients and the age range was 18-90 years; and iv) the patients did not receive any treatment prior to enrollment in the present study. The healthy individuals were diagnosed as healthy by physical examination and medical diagnosis. The exclusion criteria for the present study were as follows: i) Patients who were in the acute phase of a disease, such as acute respiratory infection, myocardial infarction, renal insufficiency or other conditions that could interfere with diagnosis; ii) patients who had severe primary disease affecting major organs, such as the heart, lungs, brain, liver, kidney or blood or any severe conditions impacting their overall survival; iii) patients who were suffering from psychiatric disorders; and iv) patients who were diagnosed with other malignant tumors. The baseline information for all participants is shown in Table I. Examples of chest CT images for lung cancer and pulmonary nodule groups can be seen in Fig. 1.

Reagents and equipment. The reagents used in the present study mainly included methanol, formic acid and ammonium acetate (supplementary material). The instruments

Table I. Baseline information of all participants.

Clinical characteristics	Pulmonary nodules group (n=28)	Lung cancer group (n=20)	Healthy group (n=20)	P-value
Age, years				
Median (range)	65.5 (44-87)	70.5 (35-82)	60.5 (48-71)	-
Mean ± SD	65.68±12.99	67.35±12.20	60.80±7.24	0.062
Sex				0.277
Male	8 (28.6)	10 (50.0)	9 (45.0)	
Female	20 (71.4)	10 (50.0)	11 (55.0)	
Smoking history				0.569
Yes	6 (21.4)	7 (35.0)	6 (30.0)	
No	22 (78.6)	13 (65.0)	14 (70.0)	
Dust exposure history				>0.999
Yes	1 (3.6)	0 (0.0)	0 (0.0)	
No	27 (96.4)	20 (100.0)	20 (100.0)	
Family history of tumors				0.057
Yes	1 (3.6)	4 (20.0)	0 (0.0)	
No	27 (96.4)	16 (80.0)	20 (100.0)	
Hypertension				0.055
Yes	5 (17.9)	5 (25.0)	0 (0.0)	
No	23 (82.1)	15 (75.0)	20 (100.0)	
Type 2 diabetes				0.061
Yes	6 (21.4)	2 (10.0)	0 (0.0)	
No	22 (78.6)	18 (90.0)	20 (100.0)	
Hyperuricemia				>0.999
Yes	1 (3.6)	0 (0.0)	0 (0.0)	
No	27 (96.4)	20 (100.0)	20 (100.0)	
Hyperlipidemia				0.059
Yes	6 (21.4)	5 (25.0)	0 (0.0)	
No	22 (78.6)	15 (75.0)	20 (100.0)	
Fatty liver				0.553
Yes	2 (7.1)	2 (10.0)	0 (0.0)	
No	26 (92.9)	18 (90.0)	20 (100.0)	
Coronary atherosclerotic heart disease				0.110
Yes	4 (14.3)	4 (20.0)	0 (0.0)	
No	24 (85.7)	16 (80.0)	20 (100.0)	
Heart failure				>0.999
Yes	1 (3.6)	0 (0.0)	0 (0.0)	
No	27 (96.4)	20 (100.0)	20 (100.0)	
Atrial fibrillation				>0.999
Yes	1 (3.6)	1 (5.0)	0 (0.0)	
No	27 (96.4)	19 (95.0)	20 (100.0)	
Cerebral infarction				>0.999
Yes	1 (3.6)	1 (5.0)	0 (0.0)	
No	27 (96.4)	19 (95.0)	20 (100.0)	
Pathological type (adenocarcinoma)	-	20 (100.0)	-	-

Values are expressed as n (%) unless otherwise specified.

used included ultra-high-performance liquid chromatograph (UHPLC), quadrupole Orbitrap ion trap mass spectrometer, ultra-pure water system, multi-tube vortex oscillator, benchtop high-speed refrigerated centrifuge, vacuum centrifugal

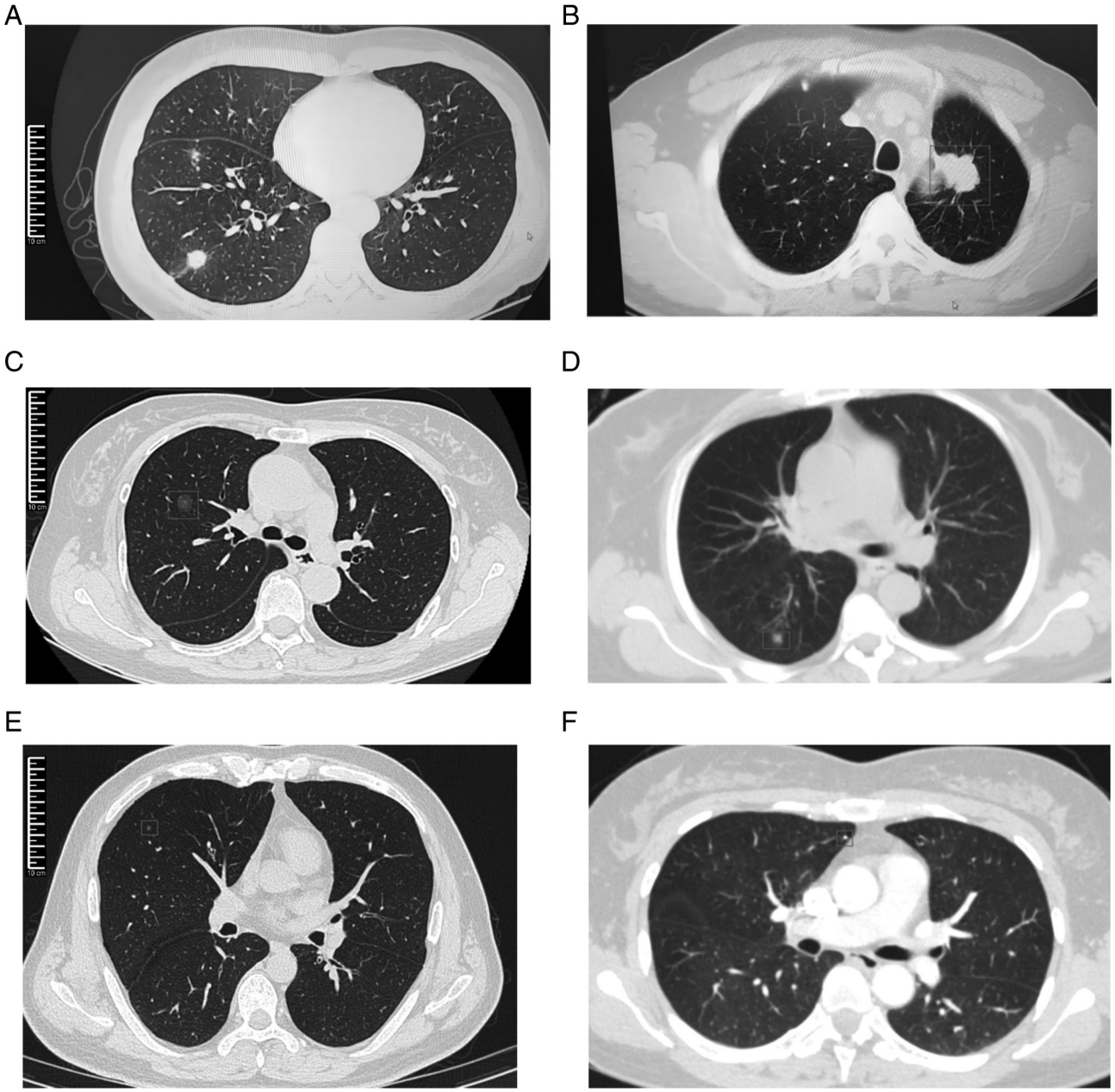

Figure 1. Examples of chest CT images for lung cancer and pulmonary nodule groups. (A) Chest CT image of a 50-year-old female patient with lung cancer. (B) Chest CT image of a 60-year-old male patient with lung cancer. (C) Chest CT image of a 63-year-old female patient with pulmonary nodule who underwent pathological examination. (D) Chest CT image of a 51-year-old female patient with pulmonary nodule who underwent pathological examination. (E) Chest CT image of a 45-year-old male patient with pulmonary nodule without pathological examination. (F) Chest CT image of a 44-year-old female patient with pulmonary nodule without pathological examination. The lesions are highlighted by red boxes in all images.

concentrator, chromatography columns, 200- and 1,000-μl pipettes, and pipette tips (Tables SI-SIII).

Plasma sample collection and preparation. A 4-ml blood sample was obtained from all of the participants in the early morning fasting state. The samples were immediately centrifuged at 1,610 x g for 10 min at 4˚C and the plasma was transferred to a 1.5-ml clean centrifuge tube and stored at -80˚C until analysis. Once all samples were collected, metabolomics analysis was conducted. The plasma samples were pretreated as follows: i) The frozen plasma samples were thawed at 4˚C for 30-60 min; ii) 100 μl of the plasma sample was precisely pipetted into a 1.5-ml centrifuge tube and three times the volume of pre-chilled methanol was added; iii) the mixture was vortexed for 5 min, allowed to sit on ice for 10 min and then centrifuged at 15,000 x g for 15 min at 4˚C; iv) 300 μl of the supernatant was collected in a centrifuge tube and vacuum-concentrated for 4 h; and v) the supernatant was re-dissolved in 50 μl of methanol/water (1:1) and vortexed for 5 min, centrifuged at 15,000 x g for 15 min at 4˚C and the supernatant was then used for analysis.

LC-MS analysis conditions. LC-MS analysis was performed on plasma samples using a Thermo Scientific Vanquish UHPLC system (Thermo Fisher Scientific, Inc.) interfaced with a heated electrospray ionization-equipped quadrupole-Orbitrap™

hybrid mass spectrometer. Chromatographic separation was performed using a Waters™ UPLC high strength silica T3 column (2.1x100 mm, 1.8 μm) under the following conditions: i) The mobile phase comprised component a) 0.1% formic acid and 0.1% aqueous formic acid solution, and component b) methanol; and ii) the flow rate was maintained at 0.3 ml/min, with the column temperature set to 40˚C and an injection volume of 1 μl was used (supplementary material).

Mass spectrometry was conducted in both positive and negative ion modes with the following specific parameters: The ion source voltage for positive and negative ions were set at 3.8 and 3.2 kV, respectively. The capillary heating temperature was 320˚C, with an auxiliary gas pressure of 10 psi and sheath gas pressure of 30 psi and the collision gas pressure was 1.5 mTorr. All gases (auxiliary, sheath and collision gas) were nitrogen. The parameters for the full scan in the first stage were set as follows: A resolution of 60,000, an automatic gain control (AGC) target of $3x10^6$, a maximum isolation time of 200 msec and a mass-to-charge ratio (m/z) scan range of 70-1,050. For metabolite identification, the dd-MS2 scan mode (a data-dependent acquisition method) was employed using the following parameters: Scanning was conducted in four segments for m/z ranges of 70-160, 150-400, 390-1,050 and 70-1,050, with a resolution of 60,000, an AGC target of $3x10^6$, a maximum isolation time of 100 msec and a maximum of 8 ion fragments to be scanned (dynamic exclusion). The mass isolation window was set to 1.5 and the collision energies were 20, 30 and 40 V. The Xcalibur software (version 4.2; Thermo Fisher Scientific, Inc.) was used to control the LC-MS system and to perform data acquisition.

Quality control (QC). QC samples were prepared for QC purposes. The QC samples were obtained by taking a fixed volume from all samples, mixing them uniformly and preparing them in the same manner as other samples. In the present study, three blank samples were used to equilibrate the chromatography column, followed by three QC samples to equilibrate the columns under the same conditions. A QC sample was inserted after every 8-10 samples to monitor the stability and reproducibility of the entire LC-MS system, ensuring the reliability of the data obtained in the present study.

Data analysis

Non-targeted metabolomics data processing. The Compound Discoverer software (version 3.3; Thermo Fisher Scientific, Inc.) was used to preprocess data in both positive and negative ion modes. The steps included importing the raw data, peak extraction, deconvolution, peak alignment and filtering or filling in missing values, resulting in an aligned peak table containing retention times, m/z and peak areas. The aligned peak table was then imported into open-source software MetaboAnalyst (version 5.0; https://www.metaboanalyst.ca/), where data filtering was performed by removing variables with a relative SD >20% in QC samples. Subsequently, normalization was carried out using the sum normalization method, followed by log data transformation and auto-scaling, ultimately producing a normalized table of retention times, m/z and peak areas. The normalized peak table was then imported into Simca (version 14.1; Umetrics, Inc.) and GraphPad Prism statistical analysis software (version 6.02; Dotmatics) for preliminary statistical analysis.

Principal component analysis (PCA) and orthogonal partial least squares-discriminant analysis (OPLS-DA) were employed to reflect overall metabolic differences and intergroup differences. To validate the accuracy of the OPLS-DA model, a permutation analysis was conducted with 200 iterations to eliminate the randomness associated with the supervised learning method. The quality of the OPLS-DA mode can be explained by R2Y and Q2 values. The R2Y estimates the goodness of fit of the model that represents the fraction of explained Y-variation and Q2 estimates the ability of prediction. Differential metabolites were identified using a combination of quantitative and qualitative methods. For the quantitative method, variable importance in the projection (VIP) values from the OPLS-DA model were used in conjunction with P-values from unpaired t-tests to identify differential metabolites, with the criteria set as VIP >1.5 and P<0.05. For the qualitative method, searches were conducted in the mzCloud (https://www.mzcloud.org), Human Metabolome Database (HMDB; http://www.hmdb.ca), ChemSpider (https://www.chemspider.com), BioCyc (https://www.biocyc.org) and Kyoto Encyclopedia of Genes and Genomes (KEGG; http://www.genome.jp/kegg) databases. The identified differential metabolites were then subjected to metabolic pathway enrichment analysis using the KEGG database, considering pathways with an impact value of ≥0.01 as significantly altered pathways.

Statistical analysis. Statistical analysis was performed using SPSS (version 25.0; IBM Corp.) and R software (version 4.4.1; Posit Software, PBC). Categorical data were described by frequency (n) and percentages (%), while continuous data were expressed as the mean ± SD. Intergroup comparisons were conducted using SPSS 25.0. The categorical data analyzed by the χ^2 test included sex and smoking history, while Fisher's exact test was applied to other categorical data. For continuous data, the age of the participants deviated from the normal distribution (tested with the Shapiro-Wilk test); therefore, the non-parametric Kruskal-Wallis test with Dunn's multiple post-hoc comparisons test was used to compare the groups. R version 4.4.1 was used for binary logistic regression analysis and receiver operating characteristic (ROC) curve analyses, with the area under the curve (AUC) used to evaluate their diagnostic effectiveness. The standard for AUC values were as follows: 0.5<AUC<0.7 indicated low diagnostic accuracy, 0.7<AUC<0.9 represented a moderate diagnostic accuracy and AUC >0.9 indicated high diagnostic accuracy. P<0.05 was considered to indicate a statistically significant difference.

Results

General characteristics of the study participants. In the present study, the lung cancer group included 10 males and 10 females, aged 35-82 years, with an average age of 67.35±12.20 years. The pulmonary nodule group consisted of 8 males and 20 females, aged 44-87 years, with an average age of 65.68±12.99 years. The healthy group included 9 males and 11 females, aged 48-71 years, with an average age of 60.80±7.24 years. After comparison, there were no significant differences among the

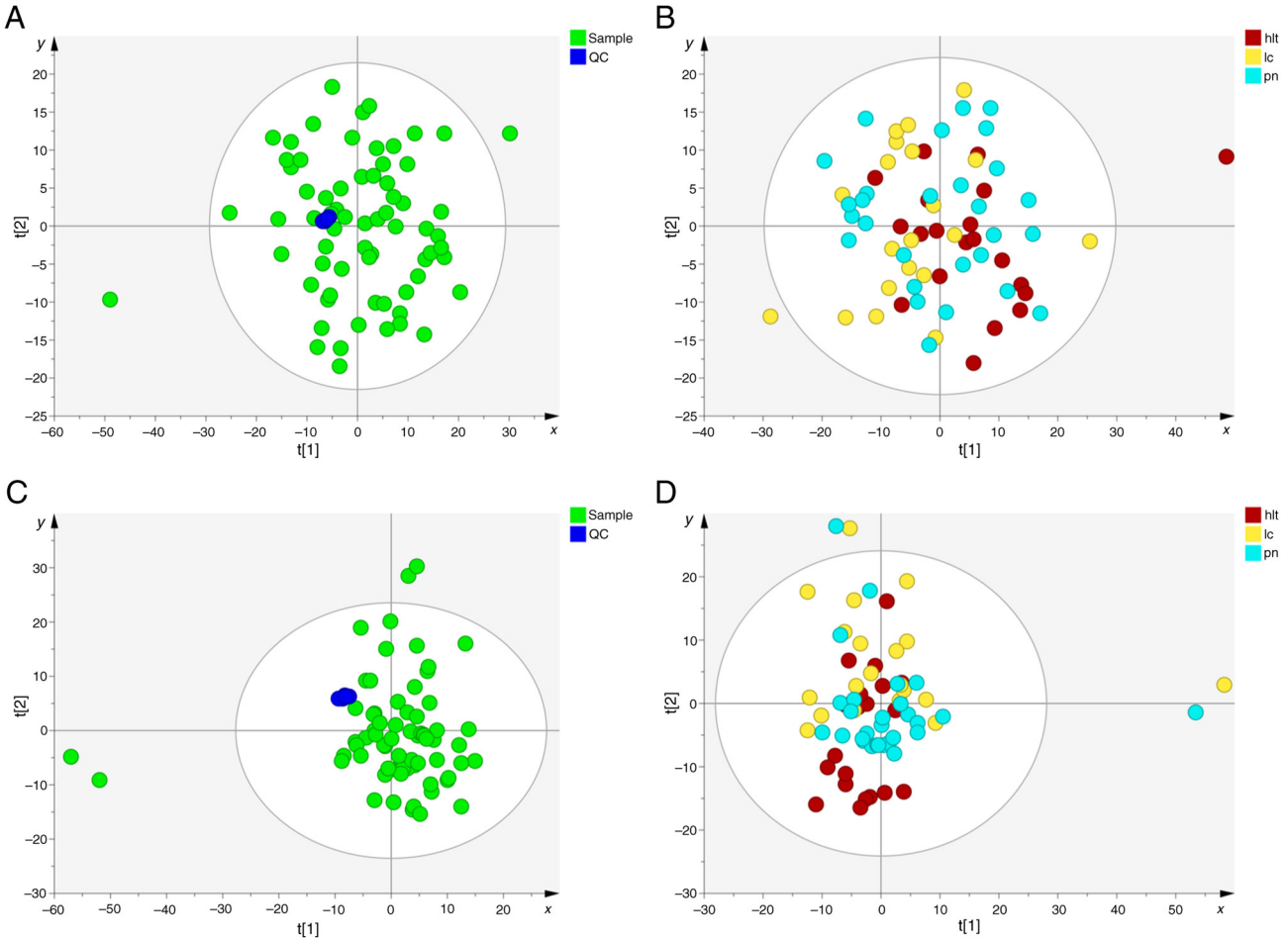

Figure 2. PCA score plots of plasma data from QC samples, pn, lc and hlt groups. (A) PCA score chart of plasma data from QC samples and other samples in the negative ion mode. (B) PCA score chart of plasma data from the pn, the lc and the hlt groups in the negative ion mode. (C) PCA score chart of plasma data from QC samples and other samples in the positive ion mode. (D) PCA score chart of plasma data from the pn, the lc and the hlt groups in the positive ion mode. Red indicates the hlt group; blue indicates the pn group; yellow indicates the lc group. PCA, principal component analysis; QC, quality control; hlt, healthy group; pn, pulmonary nodule group; lc, lung cancer group.

three groups in terms of age, sex, smoking history, dust exposure history, family history of tumors, hypertension, type 2 diabetes, hyperuricemia, hyperlipidemia, fatty liver, coronary atherosclerotic heart disease, heart failure, atrial fibrillation and cerebral infarction (P<0.05; Table I).

QC assessment and overall metabolomic characteristics among the three groups of samples. First, PCA analysis was performed to assess the quality of the QC samples and other clinical samples (Fig. 2). The results demonstrated that all QC samples clustered together under both positive and negative ion modes, indicating good system stability and reproducibility (Fig. 2A and C). Subsequently, PCA analysis was conducted on samples from the lung cancer, pulmonary nodule and healthy groups. The PCA score plots indicated a slight separation trend among the three groups (Fig. 2B and D). Lastly, to further elucidate this distinction, OPLS-DA analysis was conducted. The results demonstrated a notable separation between the pulmonary nodule and healthy groups, lung cancer and healthy groups, as well as between the pulmonary nodule and lung cancer groups, across both positive and negative ion modes, indicating notable metabolic differences among the groups (Figs. 3-5).

Differential metabolite selection among the lung cancer, pulmonary nodule and healthy groups. Differential metabolites were selected based on the VIP values and P-values from the OPLS-DA analysis. The results indicated that under both positive and negative ion modes, a total of 50 differential metabolites were identified among the lung cancer, lung nodule and healthy control groups. Among them, 35 differential metabolites were identified between the pulmonary nodule and healthy groups (Fig. 6A), 31 differential metabolites were identified between the lung cancer and healthy groups (Fig. 6B) and 14 differential metabolites were identified between the pulmonary nodule and lung cancer groups (Fig. 6C).

By comparing the differential metabolites among the groups, 18 overlapping differential metabolites were identified between the pulmonary nodule and healthy groups, as well as between the lung cancer and healthy groups, with 16 of these demonstrating the same trend of change in both comparisons. This reflected the clinical similarities between patients with pulmonary nodules and those with lung cancer. In addition, there were 11 overlapping differential metabolites between the pulmonary nodule and healthy groups, as well as between the pulmonary nodule and lung cancer groups. Furthermore, there were three overlapping differential metabolites between

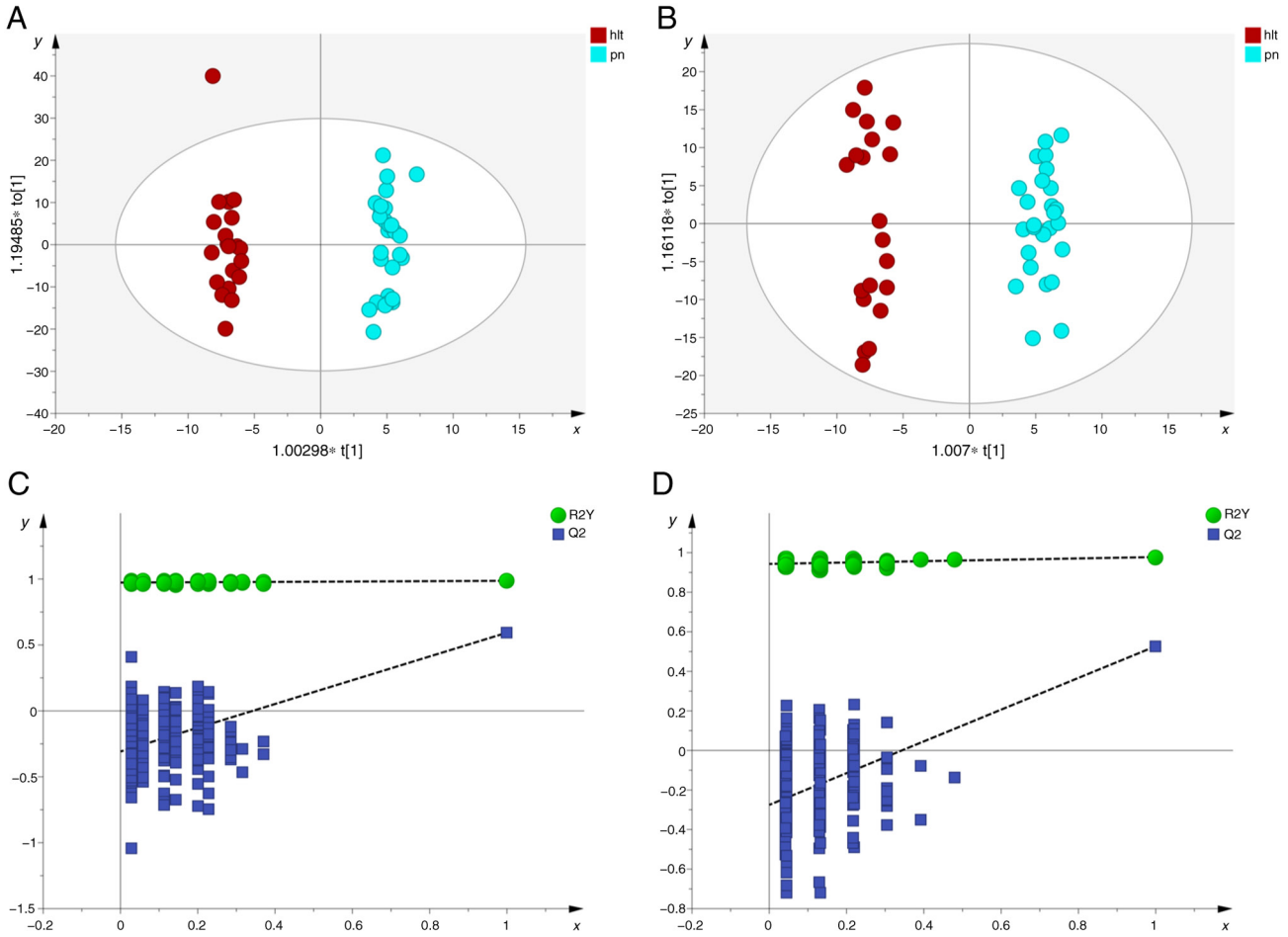

Figure 3. OPLS-DA score scatter plots and permutation test plots of plasma data from the pn and the hlt groups. (A and B) OPLS-DA score scatter plots in (A) negative ion mode (R2Y=0.986, Q2=0.593) and (B) positive ion mode (R2Y=0.978, Q2=0.527). (C and D) permutation test plots of OPLS-DA in the (C) negative ion mode (intercept of Q2 with the y-axis, -0.308) and (D) positive ion mode (intercept of Q2 with the y-axis, -0.275). R2Y estimates the goodness of fit of the model that represents the fraction of explained Y-variation and Q2 estimates the ability of prediction. OPLS-DA, orthogonal partial least squares-discriminant analysis; hlt, healthy group; pn, pulmonary nodule group; lc, lung cancer group.

the lung cancer and healthy groups, as well as between the pulmonary nodule and lung cancer group. The Venn diagram indicates the overlap of the differential metabolites in the three comparisons (Fig. 6D). Detailed information on the overlapping metabolites is provided in Table II.

Potential diagnostic biomarker selection. ROC curve analysis was conducted to assess the diagnostic value of plasma metabolites among patients with lung cancer, pulmonary nodules and healthy individuals, in order to identify potential diagnostic biomarkers. The results indicated that the AUC values for all differential metabolites between the pulmonary nodule and healthy groups, as well as between the lung cancer and healthy groups, were <0.9, suggesting that the diagnostic value of single differential metabolites was low. Further combination analysis of differential metabolites revealed that in the pulmonary nodule and healthy groups, the joint detection of pyroglutamic acid, 2-hydroxyhexadecanoylcarnitine, pantothenic acid and urocanic acid achieved an AUC value of 0.902 (95% CI, 0.807-0.996), indicating a high diagnostic value, with sensitivity and specificity of 89.3 and 90.0%, respectively (Fig. 7A). In the lung cancer and healthy groups, the combined detection of 3-methoxytyrosine, pantothenic acid and 2-hydroxyhexadecanoylcarnitine resulted in an AUC value of 0.945 (95% CI, 0.883-1.000), also indicating a high diagnostic value, with sensitivity and specificity of 90.0 and 80.0%, respectively (Fig. 7B). Of note, urocanic acid, pyroglutamic acid, pantothenic acid, 3-methoxytyrosine and 2-hydroxyhexadecanoylcarnitine were overlapping differential metabolites between the pulmonary nodule and the healthy groups, as well as between the lung cancer and the healthy groups, displaying the same trend of change. This suggested that these differential metabolites may serve as biomarkers to distinguish patients with lung cancer and pulmonary nodules from healthy individuals.

Furthermore, ROC curve analysis was conducted between the lung cancer and the pulmonary nodule groups to identify potential diagnostic biomarkers that can differentiate between patients with lung cancer and those with pulmonary nodules. The results demonstrated that the AUC value for dodecanedioic acid was 0.936 (95% CI, 0.862-1.000), indicating a high diagnostic value, with a sensitivity of 95.0% and specificity of 85.7% (Fig. 7C). This suggested that dodecanedioic acid has potential clinical application value in screening for lung cancer and pulmonary nodules and can serve as an effective biomarker to distinguish between the two.

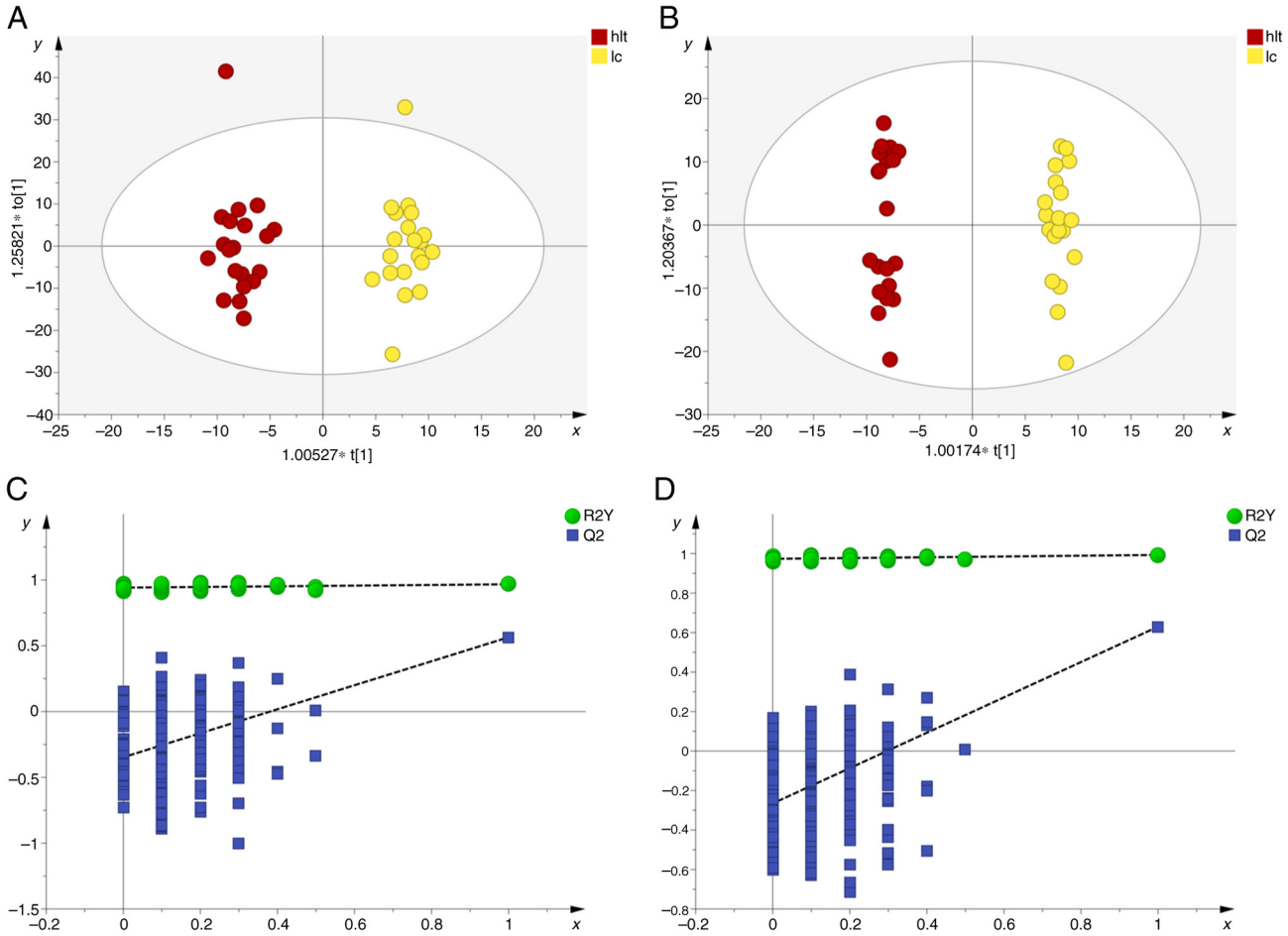

Figure 4. OPLS-DA score scatter plots and permutation test plots of plasma data from the lc and the hlt groups. (A and B) OPLS-DA score scatter plots in (A) negative ion mode (R2Y=0.967, Q2=0.564) and (B) positive ion mode (R2Y=0.993, Q2=0.630). (C and D) permut ation test plots of OPLS-DA in (C) negative ion mode (intercept of Q2 with the y-axis, -0.347) and (D) positive ion mode (intercept of Q2 with the y-axis, -0.265). R2Y estimates the goodness of fit of the model that represents the fraction of explained Y-variation and Q2 estimates the ability of prediction. OPLS-DA, orthogonal partial least squares-discriminant analysis; hlt, healthy group; pn, pulmonary nodule group; lc, lung cancer group.

Metabolic pathway analysis. Pathway enrichment analysis was performed on the selected differential metabolites. The results demonstrated that a total of 21 metabolic pathways were enriched in both the pulmonary nodules and healthy groups, among which 9 pathways exhibited significant changes, including 'linoleic acid metabolism', 'caffeine metabolism', 'histidine metabolism', 'α-linolenic acid metabolism', 'arginine biosynthesis', 'tryptophan metabolism', 'arginine and proline metabolism', 'glycerophospholipid metabolism' and 'pyrimidine metabolism' (Fig. 8A). As compared with the healthy group, a total of 18 metabolic pathways were enriched in the lung cancer group, with 9 pathways demonstrating significant changes: 'Linoleic acid', 'α-linolenic acid metabolism', 'tryptophan metabolism', 'arginine and proline metabolism', 'histidine metabolism', 'cysteine and methionine metabolism', 'arginine biosynthesis', 'citrate cycle [tricarboxylic acid (TCA) cycle]' and 'alanine, aspartate and glutamate metabolism' (Fig. 8B). In the comparison between the pulmonary nodule and lung cancer groups, a total of 10 metabolic pathways were enriched, with 3 pathways demonstrating notable changes: 'Citrate cycle (TCA cycle)', 'alanine, aspartate and glutamate metabolism' and 'arginine and proline metabolism' (Fig. 8C).

By comparing the metabolic pathways among the groups, it was identified that between the pulmonary nodule and healthy groups, as well as between the lung cancer and healthy groups, six metabolic pathways were shared: 'Linoleic acid metabolism', 'α-linolenic acid metabolism', 'tryptophan metabolism', 'arginine and proline metabolism', 'histidine metabolism' and 'arginine biosynthesis'. Between the pulmonary nodule and healthy groups, as well as between the pulmonary nodule and lung cancer groups, arginine and proline metabolism was a shared and significantly altered pathway. In addition, between the lung cancer and healthy groups, as well as between the pulmonary nodule and lung cancer groups, three metabolic pathways were shared: 'Citrate cycle (TCA cycle)', 'alanine, aspartate and glutamate metabolism' and 'arginine and proline metabolism'. Furthermore, the present study revealed that 'arginine and proline metabolism' is a pathway that indicated significant changes across all three groups.

Discussion

Lung cancer staging is a key determinant of prognosis (7). Several countries, such as the USA and the UK, have implemented lung cancer screening programs aimed at improving

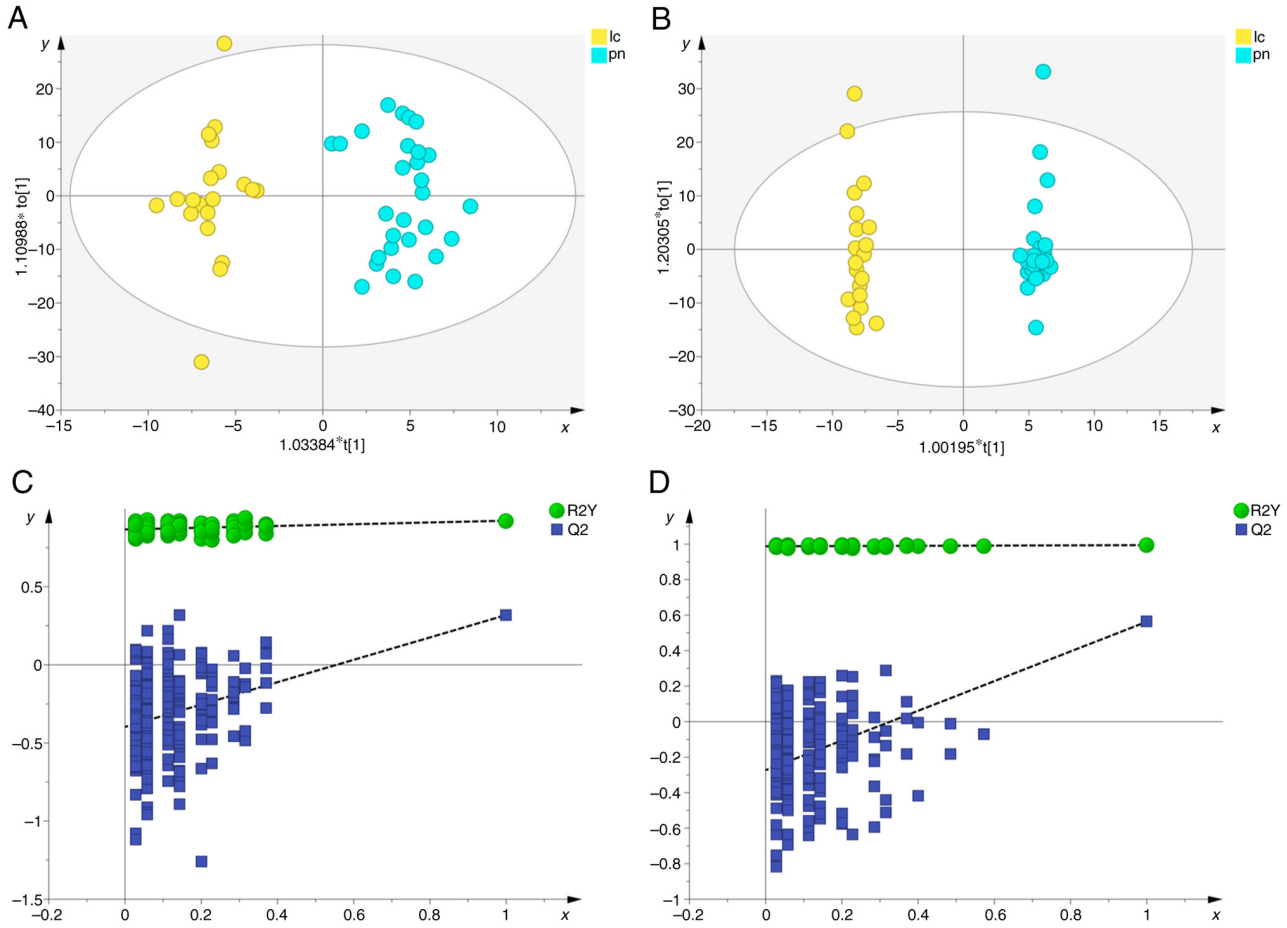

Figure 5. OPLS-DA score scatter plots and permutation test plots of plasma data from the pn and the lc groups. (A and B) OPLS-DA score scatter plots in (A) negative ion mode (R2Y=0.994, Q2=0.319) and (B) positive ion mode (R2Y=0.922, Q2=0.563). (C and D) permutation test plots of OPLS-DA in (C) negative ion mode (intercept of Q2 with the y-axis, -0.398) and (D) positive ion mode (intercept of Q2 with the y-axis, -0.274). OPLS-DA, orthogonal partial least squares-discriminant analysis; hlt, healthy group; pn, pulmonary nodule group; lc, lung cancer group. R2Y estimates the goodness of fit of the model that represents the fraction of explained Y-variation and Q2 estimates the ability of prediction.

outcomes through early diagnosis (23-25). CT, as the primary screening tool, offers rich morphological information, high sensitivity and technical maturity (10,26). However, its specificity is relatively low, as certain benign lesions share imaging characteristics with lung cancer, leading to overdiagnosis (27). To address this limitation, current research focuses on multimodal strategies and the development of novel methods. For example, using artificial intelligence to mine radiomic features and integrate multimodal data to enhance CT specificity (5,27). Metabolomics is an emerging technology and analyzes metabolites (15). As the products of interactions among genes, RNA and proteins, metabolites can reflect the current physiological and pathological states of the body in real time (28) and have the potential for high specificity, offering a novel avenue to improve the diagnostic specificity of lung cancer in the future. In the present study, LC-MS was used to identify specific metabolic biomarkers that distinguish lung cancer, pulmonary nodules and healthy individuals, providing a novel strategy for early diagnosis.

The differential metabolites and ROC curves from the present study demonstrated that urocanic acid, pyroglutamic acid, pantothenic acid, 3-methoxytyrosine and 2-hydroxyhexadecanoylcarnitine display the same trend of changes in lung cancer, pulmonary nodules and healthy individuals. In addition, dodecanedioic acid can distinguish between pulmonary nodule and lung cancer, suggesting that the aforementioned metabolites are involved in the occurrence and development of lung cancer. This is consistent with previous literature. Filaggrin is degraded into histidine, which is then converted into urocanic acid by histidinase. Urocanic acid undergoes a series of enzymatic reactions to form glutamic acid (29-31). The glutamic acid is subsequently metabolized into pyroglutamic acid, which influences glutamine and glutathione metabolism, thereby participating in tumorigenesis (32,33). Pantothenic acid is a precursor of coenzyme A, which is acetylated to form acetyl-coenzyme A (acetyl-CoA), participating in processes such as the TCA cycle and lipid metabolism, thereby affecting the growth and proliferation of cancer (34-36). The HMDB indicates that 3-methoxytyrosine is a tyrosine-derived metabolite, while 2-hydroxyhexadecanoylcarnitine is classified as a member of fatty acid esters. Dysregulation of tyrosine metabolism can not only lead to lung cancer but also interplay with the tumor immune microenvironment, which serves a key role in cancer development (37-39). In addition, it has been reported that 3-methoxytyrosine may regulate immune responses by modulating enzyme activity (40) and these immune responses are closely associated with tumorigenesis and progression (41,42).

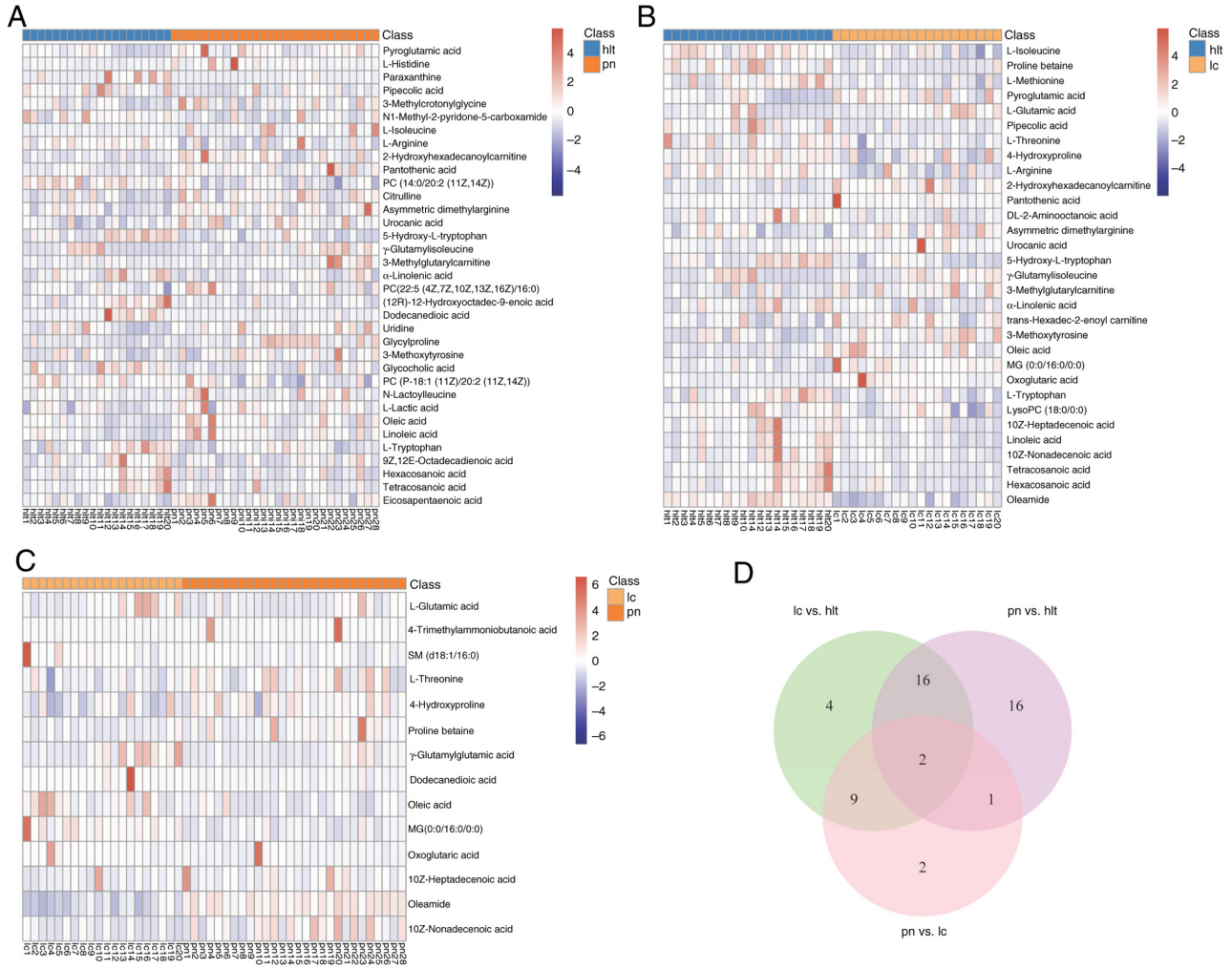

Figure 6. Heatmap and Venn diagram of differential metabolites. (A) Heatmap of differential metabolites for the pn and the hlt groups. (B) Heatmap of differential metabolites for the lc and the hlt groups. (C) Heatmap of differential metabolites for the pn and the lc groups. (D) Venn diagram of the differential metabolites of the three comparisons. In the heatmap, blue represents downregulation and red represents upregulation. hlt, healthy group; pn, pulmonary nodule group; lc, lung cancer group.

Fatty acid esters are derivatives of fatty acids, and fatty acids can then feed into various metabolic pathways, such as the synthesis of complex lipids like triacylglycerides, and participation in β-oxidation processes, providing energy for tumor proliferation and producing intermediate products that connect different metabolic activities (43). This is a key factor in the occurrence of cancer (44). Dodecanedioic acid, a ^{12}C/medium-chain water-soluble dicarboxylic acid, undergoes oxidative metabolism in mitochondria to generate acetyl-CoA (45). Acetyl-CoA provides substrates and raw materials for fatty acid synthesis and histone acetylation modification, which are key pathways in the occurrence and progression of cancer (46,47). Therefore, the present study suggested that urocanic acid, pyroglutamic acid, pantothenic acid, 3-methoxytyrosine and 2-hydroxyhexadecanoylcarnitine can serve as biomarkers to distinguish patients with lung cancer from those with pulmonary nodules and healthy individuals. Dodecanedioic acid is a potential biomarker for early lung cancer diagnosis of patients with pulmonary nodule. To the best of our knowledge, the results of the present study are novel and have not been covered in previous studies. Compared with the high-abundance metabolites detected by NMR, such as lipoproteins and glucose and the volatile metabolites identified by GC-MS, such as naphthalene and propene, the LC-MS employed in the present study detected certain different metabolites, including small molecular organic acids, acylcarnitines and modified amino acids, expanding the metabolic profile of lung cancer (48-50).

The findings from the metabolic pathway enrichment analysis demonstrated that there are notable abnormalities in pathways associated with amino acids and lipids among lung cancer, pulmonary nodules and healthy individuals. This suggested that the mechanisms underlying the development of lung cancer may be associated with these two metabolic alterations. Research has revealed that metabolic reprogramming of amino acids and lipids represents a hallmark of tumorigenesis (51,52). Amino acids, as components of proteins and signaling molecules, serve a role in various biological processes, including the biosynthesis of proteins and nucleic acids, energy production, oxidative stress homeostasis and epigenetic modifications (51,53). These biological processes established favorable conditions for the occurrence of tumors. For instance, amino acids, such as glycine and aspartate, provide carbon and nitrogen for purine synthesis in cancer

Table II. Differential metabolites with common metabolic characteristics across groups.

Pulmonary nodules and healthy groups vs. lung cancer and healthy groups (n=18)	Lung cancer and healthy groups vs. pulmonary nodules and lung cancer groups (n=11)	Pulmonary nodules and healthy groups vs. pulmonary nodules and lung cancer groups (n=3)
Pyroglutamic acid	Oxoglutaric acid	Oleic acid
2-Hydroxyhexadecanoylcarnitine	MG(0:0/16:0/0:0)	γ-Glutamylisoleucine
Pantothenic acid	L-glutamic acid	Dodecanedioic acid
Asymmetric dimethylarginine	L-threonine	-
Urocanic acid	4-Hydroxyproline	-
γ-Glutamylisoleucine	Proline betaine	-
3-Methylglutarylcarnitine	10z-Heptadecenoic acid	-
3-Methoxytyrosines	Oleamide	-
Oleic acid	10z-Nonadecenoic acid	-
L-isoleucine	Oleic acid	-
Linoleic acid	γ-Glutamylisoleucine	-
5-Hydroxy-L-tryptophan	-	-
α-Linolenic acid	-	-
L-Tryptophan	-	-
Hexacosanoic acid	-	-
Tetracosanoic acid	-	-
L-arginine	-	-
Pipecolic acid	-	-

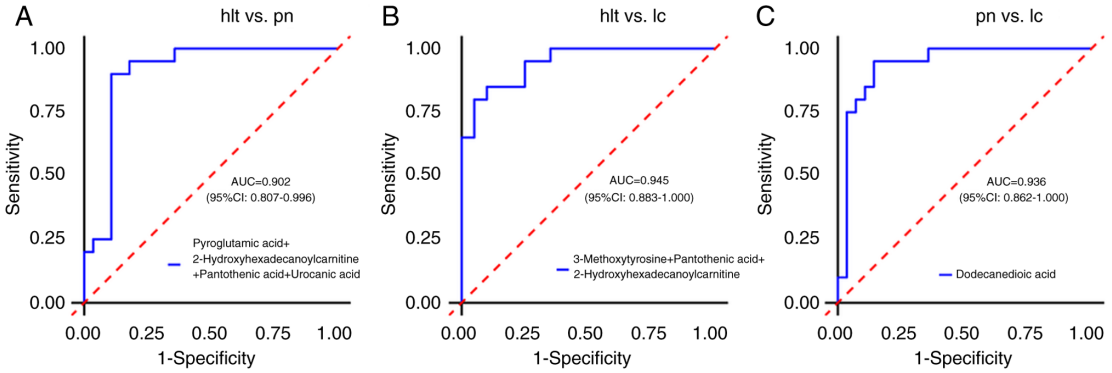

Figure 7. ROC curves of differential metabolites. (A) ROC curve for distinguishing between the pn and hlt groups based on pyroglutamic acid, 2-hydroxyhexadecanoylcarnitine, pantothenic acid and urocanic acid. (B) ROC curve for distinguishing between the lc and hlt groups based on 3-methoxytyrosine, pantothenic acid and 2-hydroxyhexadecanoylcarnitine. (C) ROC curve for distinguishing between the pn and lc groups based on dodecanedioic acid. ROC, receiver operating characteristic; hlt, healthy group; pn, pulmonary nodule group; lc, lung cancer group; AUC, area under the curve.

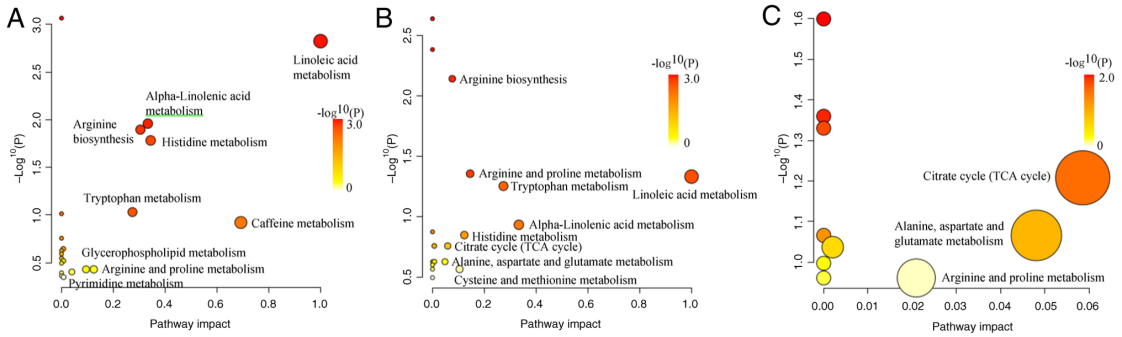

Figure 8. Bubble plot of KEGG pathway analysis. (A) Bubble plot of KEGG pathway analysis for the pn and the hlt groups. (B) Bubble plot of KEGG pathway analysis for the lc and the hlt groups. (C) Bubble plot of KEGG pathway analysis for the pn and the lc groups. KEGG, Kyoto Encyclopedia of Genes and Genomes; hlt, healthy group; pn, pulmonary nodule group; lc, lung cancer group. Node color and radius are based on the P-value and pathway impact value, respectively. The larger the circle is, the larger the influence factor is. The deeper red color has the larger value of- log(p), which means the more significant enrichment.

cells (54); glutamine metabolism can drive the TCA cycle to maintain mitochondrial ATP production, supplying energy to cancer cells (55); and tryptophan metabolism through the kynurenine pathway mediates tumor immune evasion (56). Lipids primarily support cancer cell energy supply and participate in cancer cell signal transduction and membrane structure formation through metabolic processes, such as re-regulated uptake and synthesis, as well as fatty acid oxidation (52,57), thereby promoting tumorigenesis. For instance, fatty acid oxidation can generate a notable amount of ATP, providing energy for the rapid proliferation of cancer cells (58,59). Increased fatty acid synthesis can meet the material requirements for cancer cell membrane generation, sustaining cancer cell proliferation (59,60). Oleic acid can promote cancer cell proliferation by inducing the activation of relevant enzymes and pathways, as well as promote the expression level of cyclin D1, facilitating the G_1-to-S phase transition in the cell cycle and accelerating cell proliferation (61). The results of the present study support and supplement previous research: A previous study on lung cancer has identified that the principal changes in metabolic pathways among healthy individuals, pulmonary nodules and lung cancer involve the amino acid metabolism (62). However, the present study identified that, in addition to changes in amino acid metabolism, lipid metabolism also underwent alterations.

Furthermore, the results of the metabolic pathway enrichment analysis emphasized the significant role of arginine and proline metabolism in the development of lung cancer. A previous study reported that arginine and proline metabolism are closely associated with glutamine metabolism, which can be utilized by cancer cells to accelerate tumor growth (63), serving as a hallmark of tumor progression. Glutamine is metabolically converted into glutamate. Glutamate can be converted to proline under the action of pyrroline-5-carboxylic acid (P5C) synthase. Proline can be converted to arginine through the intermediate P5C and arginine, under the hydrolysis of arginase, generates urea and ornithine (63,64). On one hand, ornithine can be transformed into citrulline by ornithine transcarbamylase and citrulline can be converted back into arginine through the urea cycle; on the other hand, it can serve as a precursor for the synthesis of proline or glutamate (63,65,66). This metabolic process forms the glutamine-arginine-proline metabolic axis, which has been shown to serve a notable role in cancer progression.

The present study, as an exploratory investigation, had two main limitations: Firstly, the sample size was relatively small, which may not fully capture the metabolic heterogeneity of the study population, leading to the potential missed detection of certain differential metabolites. Secondly, although ROC analysis indicated that the metabolic biomarkers in the present study have good diagnostic efficacy, the current results have not yet been validated in independent cohorts and their clinical applicability requires further investigation. In the future, our group plans to conduct multi-center, large-sample studies to systematically validate the clinical applicability and generalizability of the present findings.

In conclusion, the present study employed LC-MS to analyze and compare the plasma metabolic profiles of patients with lung cancer, pulmonary nodules and healthy individuals. Strict filtration criteria were applied to select differential metabolites and potential biomarkers. A total of 50 differential metabolites were identified, which were enriched in pathways associated with amino acid and lipid metabolism, including 'linoleic acid metabolism', 'α-linolenic acid metabolism', 'arginine and proline metabolism' and others. The ROC curve analysis identified six potential biomarkers with good sensitivity and specificity to distinguish lung cancer, pulmonary nodules and healthy individuals, including urocanic acid, pyroglutamic acid, pantothenic acid, 3-methoxytyrosine, 2-hydroxyhexadecanoylcarnitine and dodecanedioic acid. Furthermore, the findings from the present study on metabolic changes in lung cancer may provide novel insights into understanding the pathophysiological mechanisms of the disease. In the future, a systematic and in-depth investigation of lung cancer by integrating proteomics, genomics and other approaches may be conducted to facilitate the practical application of potential biomarkers.

Acknowledgements

Not applicable.

Funding

The Clinical Scientific Research Fund for Central High-Level Traditional Chinese Medicine Hospitals [grant no. DZMG-TZZX-24005 and the present study was supported by the Special Fund for Fundamental Research of Central Universities (grant no. 2022-JYB-JBZR-029)].

Availability of data and materials

The data generated in the present study may be found in the Metabolights database under accession no. MTBLS12985 or using the following URL: https://ftp.ebi.ac.uk/pub/databases/metabolights/studies/public/MTBLS12985/).

Authors' contributions

YLiu acquired the data, conceived and designed the present study and revised the final version of the manuscript. YangL analyzed the data, conceived and designed the present study, and wrote the manuscript. HH acquired the data. YD, HT, YZ and JZ collected plasma from enrolled volunteers. KL read the chest CT of enrolled volunteers and collected data. YLi and FS designed the present study and confirm the authenticity of all the raw data. FS acquired the data and conceived the study. All authors have read and approved the final manuscript.

Ethics approval and consent to participate

The present study was reviewed and approved by the Ethical Committee of Dongzhimen Hospital of Beijing University of Chinese Medicine (approval no. 2022DZMEC-312-02; Beijing, China). All participants were fully informed of the study and gave their written informed consent before participation in the present study. The present study was conducted in accordance with the Declaration of Helsinki.

Patient consent for publication

Not applicable.

Competing interests

The authors declare that they have no competing interests.

Use of artificial intelligence tools

During the preparation of this work, artificial intelligence tools (OpenAI and their language model, chatGPt 4.0) were used to improve the readability and language of the manuscript or to generate images, and subsequently, the authors revised and edited the content produced by the artificial intelligence tools as necessary, taking full responsibility for the ultimate content of the present manuscript.

References

1. Sung H, Ferlay J, Siegel RL, Laversanne M, Soerjomataram I, Jemal A and Bray F: Global Cancer Statistics 2020: GLOBOCAN Estimates of Incidence and Mortality Worldwide for 36 Cancers in 185 countries. CA Cancer J Clin 71: 209-249, 2021.
2. Thai AA, Solomon BJ, Sequist LV, Gainor JF and Heist RS: Lung cancer. Lancet 398: 535-554, 2021.
3. Bi H, Yin L, Fang W, Song S, Wu S and Shen J: Association of CEA, NSE, CYFRA 21-1, SCC-Ag, and ProGRP with Clinicopathological characteristics and chemotherapeutic outcomes of lung cancer. Lab Med 54: 372-379, 2023.
4. Wang Y, Guo Q, Huang Z, Song L, Zhao F, Gu T, Feng Z, Wang H, Li B, Wang D, *et al*: Cell-free epigenomes enhanced fragmentomics-based model for early detection of lung cancer. Clin Transl Med 15: e70225, 2025.
5. Zhang C, Li J, Huang J and Wu S: Computed tomography image under convolutional neural network deep learning algorithm in pulmonary nodule detection and lung function examination. J Healthc Eng 2021: 3417285, 2021.
6. Liang J, Ye G, Guo J, Huang Q and Zhang S: Reducing False-positives in lung nodules detection using balanced datasets. Front Public Health 9: 671070, 2021.
7. Wu Z, Wang F, Cao W, Qin C, Dong X, Yang Z, Zheng Y, Luo Z, Zhao L, Yu Y, *et al*: Lung cancer risk prediction models based on pulmonary nodules: A systematic review. Thorac Cancer 13: 664-677, 2022.
8. Zheng J, Hao Y, Guo Y, Du M, Wang P and Xin J: An 18F-FDG-PET/CT-based radiomics signature for estimating malignance probability of solitary pulmonary nodule. Clin Respir J 18: e13751, 2024.
9. Zhu K, Tang S, Pan D, Wang X, Xu Y, Yan J, Wang L, Chen C and Yang M: Development and biological evaluation of a novel CEACAM6-targeted PET tracer for distinguishing malignant nodules in early-stage lung adenocarcinoma. Eur J Nucl Med Mol Imaging 52: 2414-2430, 2025.
10. Nooreldeen R and Bach H: Current and future development in lung cancer diagnosis. Int J Mol Sci 22: 8661, 2021.
11. Wang X, Chen Y, Ma C, Bi L, Su Z, Li W and Wang Z: Current advances and future prospects of blood-based techniques for identifying benign and malignant pulmonary nodules. Crit Rev Oncol Hematol 207: 104608, 2025.
12. Wang CF, Peng SJ, Liu RQ, Yu YJ, Ge QM, Liang RB, Li QY, Li B and Shao Y: The combination of CA125 and NSE is useful for predicting liver metastasis of lung cancer. Dis Markers 2020: 8850873, 2020.
13. Anwardeen NR, Diboun I, Mokrab Y, Althani AA and Elrayess MA: Statistical methods and resources for biomarker discovery using metabolomics. BMC Bioinformatics 24: 250, 2023.
14. Wang S, He T and Wang H: Non-targeted metabolomics study for discovery of hepatocellular carcinoma serum diagnostic biomarker. J Pharm Biomed Anal 239: 115869, 2024.
15. Huang X, Chen L, Liu L, Chen H, Gong Z, Lyu J, Li Y, Jiang Q, Zeng X, Zhang P and Zhou H: Untargeted metabolomics analysis reveals the potential mechanism of imatinib-induced skin rash in patients with gastrointestinal stromal tumor. Int Immunopharmacol 140: 112728, 2024.
16. Johnson CH, Ivanisevic J and Siuzdak G: Metabolomics: Beyond biomarkers and towards mechanisms. Nat Rev Mol Cell Biol 17: 451-459, 2016.
17. Xu K, Berthiller F, Metzler-Zebeli BU and Schwartz-Zimmermann HE: Development and validation of targeted metabolomics methods using liquid Chromatography-tandem mass spectrometry (LC-MS/MS) for the quantification of 235 plasma metabolites. Molecules 30: 706, 2025.
18. Wang R, Hu Q, Wu Y, Guan N, Han X and Guan X: Intratumoral lipid metabolic reprogramming as a pro-tumoral regulator in the tumor milieu. Biochim Biophys Acta Rev Cancer 1878: 188962, 2023.
19. Rispoli MG, Valentinuzzi S, De Luca G, Del Boccio P, Federici L, Di Ioia M, Digiovanni A, Grasso EA, Pozzilli V, Villani A, *et al*: Contribution of metabolomics to multiple sclerosis diagnosis, prognosis and treatment. Int J Mol Sci 22: 11112, 2021.
20. Liang S, Cao X, Wang Y, Leng P, Wen X, Xie G, Luo H and Yu R: Metabolomics analysis and diagnosis of lung cancer: Insights from diverse sample types. Int J Med Sci 21: 234-252, 2024.
21. Tang Y, Li Z, Lazar L, Fang Z, Tang C and Zhao J: Metabolomics workflow for lung cancer: Discovery of biomarkers. Clin Chim Acta 495: 436-445, 2019.
22. Chelala L, Hossain R, Kazerooni EA, Christensen JD, Dyer DS and White CS: Lung-RADS version 1.1: Challenges and a look ahead, from the AJR special series on radiology reporting and data systems. AJR Am J Roentgenol 216: 1411-1422, 2021.
23. Aunger J, Yip KP, Dosanjh K, Scandrett K, Ungureanu B, Newnham M and Turner AM: Interventions to improve adherence to clinical guidelines for the management and Follow-Up of pulmonary nodules: A systematic review. Chest 168: 248-268, 2025.
24. Kramer BS, Berg CD, Aberle DR and Prorok PC: Lung cancer screening with Low-dose helical CT: Results from the national lung screening Trial (NLST). J Med Screen 18: 109-111, 2011.
25. O Reilly D, Roche S, Noonan C, O'Shea J, Toomey S, Hennessy BT, Fitzmaurice GJ, Egan K, Dunne J, Dowling CM, *et al*: Lung health check pilot: Ireland's flagship lung cancer screening trial. BMJ Open Respir Res 12: e003035, 2025.
26. Zhao Y, Wang Z, Liu X, Chen Q, Li C, Zhao H and Wang Z: Pulmonary nodule detection based on multiscale feature fusion. Comput Math Methods Med 2022: 8903037, 2022.
27. Zhu J, Tao J, Zhu M, Liu J, Ma C, Chen K, Wang Y, Lu X, Saito Y and Ni B: Development and validation of CT radiomics diagnostic models: Differentiating benign from malignant pulmonary nodules and evaluating malignancy degree. J Thorac Dis 17: 1645-1672, 2025.
28. Xu L, Chang C, Jiang P, Wei K, Zhang R, Jin Y, Zhao J, Xu L, Shi Y, Guo S, *et al*: Metabolomics in rheumatoid arthritis: Advances and review. Front Immunol 13: 961708, 2022.
29. Pham DL, Lim KM, Joo KM, Park HS, Leung DYM and Ye YM: Increased cis-to-trans urocanic acid ratio in the skin of chronic spontaneous urticaria patients. Sci Rep 7: 1318, 2017.
30. Wang L, Tan Y, Wang H, Yu XD, Mo Y, Reilly J, He Z and Shu X: Urocanic acid facilitates acquisition of object recognition memory in mice. Physiol Behav 266: 114201, 2023.
31. Hart PH and Norval M: The multiple roles of urocanic acid in health and disease. J Invest Dermatol 141: 496-502, 2021.
32. Mi M, Liu Z, Zheng X, Wen Q, Zhu F, Li J, Mungur ID and Zhang L: Serum metabolomic profiling based on GC/MS helped to discriminate diffuse large B-cell lymphoma patients with different prognosis. Leuk Res 111: 106693, 2021.
33. Vidman L, Zheng R, Bodén S, Ribbenstedt A, Gunter MJ, Palmqvist R, Harlid S, Brunius C and Van Guelpen B: Untargeted plasma metabolomics and risk of colorectal cancer-an analysis nested within a large-scale prospective cohort. Cancer Metab 11: 17, 2023.
34. Peterson CT, Rodionov DA, Osterman AL and Peterson SN: B vitamins and their role in immune regulation and cancer. Nutrients 12: 3380, 2020.
35. Hrubša M, Siatka T, Nejmanová I, Vopršalová M, Kujovská Krčmová L, Matoušová K, Javorská L, Macáková K, Mercolini L, Remião F, *et al:* Biological properties of vitamins of the B-Complex, part 1: Vitamins B1, B2, B3, and B5. Nutrients 14: 484, 2022.
36. Chen G, Bao B, Cheng Y, Tian M, Song J, Zheng L and Tong Q: Acetyl-CoA metabolism as a therapeutic target for cancer. Biomed Pharmacother 168: 115741, 2023.
37. Zhou Y, Li X, Long G, Tao Y, Zhou L and Tang J: Identification and validation of a tyrosine metabolism-related prognostic prediction model and characterization of the tumor micro-environment infiltration in hepatocellular carcinoma. Front Immunol 13: 994259, 2022.

38. Wang X, Chen Y, Lan B, Wang Y, Lin W, Jiang X, Ye J, Shang B, Feng C, Liu J, *et al*: Heterogeneity of tyrosine-based melanin anabolism regulates pulmonary and cerebral organotropic colonization microenvironment of melanoma cells. Theranostics 12: 2063-2079, 2022.
39. Wu T and Dai Y: Tumor microenvironment and therapeutic response. Cancer Lett. 387: 61-68, 2017.
40. Zou X, Huang H and Tan Y: Genetically determined metabolites in allergic conjunctivitis: A Mendelian randomization study. World Allergy Organ J 17: 100894, 2024.
41. Yang L, Chu Z, Liu M, Zou Q, Li J, Liu Q, Wang Y, Wang T, Xiang J and Wang B: Amino acid metabolism in immune cells: Essential regulators of the effector functions, and promising opportunities to enhance cancer immunotherapy. J Hematol Oncol 16: 59, 2023.
42. Zhang Z, Hu Y, Chen Y, Chen Z, Zhu Y, Chen M, Xia J, Sun Y and Xu W: Immunometabolism in the tumor microenvironment and its related research progress. Front Oncol 12: 1024789, 2022.
43. Koundouros N and Poulogiannis G: Reprogramming of fatty acid metabolism in cancer. Br J Cancer 122: 4-22, 2020.
44. Broadfield LA, Pane AA, Talebi A, Swinnen JV and Fendt SM: Lipid metabolism in cancer: New perspectives and emerging mechanisms. Dev Cell 56: 1363-1393, 2021.
45. Radzikh I, Fatica E, Kodger J, Shah R, Pearce R and Sandlers YI: Metabolic outcomes of anaplerotic dodecanedioic acid supplementation in very long Chain Acyl-CoA dehydrogenase (VLCAD) deficient fibroblasts. Metabolites 11: 538, 2021.
46. He W, Li Q and Li X: Acetyl-CoA regulates lipid metabolism and histone acetylation modification in cancer. Biochim Biophys Acta Rev Cancer 1878: 188837, 2023.
47. Feron O: The many metabolic sources of acetyl-CoA to support histone acetylation and influence cancer progression. Ann Transl Med 7 (Suppl 8): S277, 2019.
48. Noreldeen HAA: Recent advances in lung cancer lipidomics: Analytical techniques and their applications. Clin Chim Acta 577: 120470, 2025.
49. Rocha CM, Carrola J, Barros AS, Gil AM, Goodfellow BJ, Carreira IM, Bernardo J, Gomes A, Sousa V, Carvalho L, *et al*: Metabolic signatures of lung cancer in biofluids: NMR-based metabonomics of blood plasma. J Proteome Res 10: 4314-4324, 2011.
50. Musharraf SG, Mazhar S, Choudhary MI, Rizi N and Atta-ur-Rahman: Plasma metabolite profiling and chemometric analyses of lung cancer along with three controls through gas chromatography-mass spectrometry. Sci Rep 5: 8607, 2015.
51. Li X and Zhang HS: Amino acid metabolism, redox balance and epigenetic regulation in cancer. FEBS J 291: 412-429, 2024.
52. Jin HR, Wang J, Wang ZJ, Xi MJ, Xia BH, Deng K and Yang JL: Lipid metabolic reprogramming in tumor microenvironment: From mechanisms to therapeutics. J Hematol Oncol 16: 103, 2023.
53. Liu X, Ren B, Ren J, Gu M, You L and Zhao Y: The significant role of amino acid metabolic reprogramming in cancer. Cell Commun Signal 22: 380, 2024.
54. Xu X, Peng Q, Jiang X, Tan S, Yang Y, Yang W, Han Y, Chen Y, Oyang L, Lin J, *et al*: Metabolic reprogramming and epigenetic modifications in cancer: From the impacts and mechanisms to the treatment potential. Exp Mol Med 55: 1357-1370, 2023.
55. Lieu EL, Nguyen T, Rhyne S and Kim J: Amino acids in cancer. Exp Mol Med 52: 15-30, 2020.
56. Greene LI, Bruno TC, Christenson JL, D'Alessandro A, Culp-Hill R, Torkko K, Borges VF, Slansky JE and Richer JK: A Role for Tryptophan-2,3-dioxygenase in CD8 T-cell suppression and evidence of tryptophan catabolism in breast cancer patient plasma. Mol Cancer Res 17: 131-139, 2019.
57. Yang K, Wang X, Song C, He Z, Wang R, Xu Y, Jiang G, Wan Y, Mei J and Mao W: The role of lipid metabolic reprogramming in tumor microenvironment. Theranostics 13: 1774-1808, 2023.
58. Snaebjornsson MT, Janaki-Raman S and Schulze A: Greasing the wheels of the cancer machine: The role of lipid metabolism in cancer. Cell Metab 31: 62-76, 2020.
59. An Q, Lin R, Wang D and Wang C: Emerging roles of fatty acid metabolism in cancer and their targeted drug development. Eur J Med Chem 240: 114613, 2022.
60. Acharya R, Shetty SS and Kumari NS: Fatty acid transport proteins (FATPs) in cancer. Chem Phys Lipids 250: 105269, 2023.
61. Zhang Y, Wang D, Lv B, Hou X, Liu Q, Liao C, Xu R, Zhang Y, Xu F and Zhang P: Oleic acid and insulin as key characteristics of T2D promote colorectal cancer deterioration in xenograft mice revealed by functional metabolomics. Front Oncol 11: 685059, 2021.
62. Yu M, Wen W, Wang Y, Shan X, Yi X, Zhu W, Aa J and Wang G: Plasma metabolomics reveals risk factors for lung adenocarcinoma. Front Oncol 14: 1277206, 2024.
63. Wang D, Duan JJ, Guo YF, Chen JJ, Chen TQ, Wang J and Yu SC: Targeting the glutamine-arginine-proline metabolism axis in cancer. J Enzyme Inhib Med Chem 39: 2367129, 2024.
64. Matos A, Carvalho M, Bicho M and Ribeiro R: Arginine and arginases modulate metabolism, tumor microenvironment and prostate cancer progression. Nutrients 13: 4503, 2021.
65. Du T and Han J: Arginine metabolism and its potential in treatment of colorectal cancer. Front Cell Dev Biol 9: 658861, 2021.
66. Niu F, Yu Y, Li Z, Ren Y, Li Z, Ye Q, Liu P, Ji C, Qian L and Xiong Y: Arginase: An emerging and promising therapeutic target for cancer treatment. Biomed Pharmacother 149: 112840, 2022.